OPTIMIZATION OF SIC COLLOIDAL INK FOR DIRECT-WRITE ADDITIVE MANUFACTURING VIA DUAL-POLYELECTROLYTE RATIO METHOD

M.A. Odunosho* and J.E. Smay*

*Department of Materials Science and Engineering, Oklahoma State University, Tulsa, OK 74106

Abstract

Robocasting is being extensively explored for fabrication of silicon carbide (SiC) components for a variety of applications. Many of the previous works have only been able to print low-to-moderate volume solid loadings (ϕ=0.33-0.44) and with larger nozzle sizes (600-1500μm) because high-solid loadings are difficult to extrude. However, printing low-moderate solid loadings and larger nozzles usually lead to poor surface finish and excessive shrinkage upon sintering of printed part. Therefore, optimizing SiC ink would be beneficial for printing high-solid loadings with smaller nozzles. In this study, a systematic approach towards the optimization of SiC by dual-polyelectrolyte ratio method was explored. A viscoelastic study revealed that lower concentration of flocculant is more suitable for SiC colloidal gel used in robocasting while higher flocculant concentration led to over-flocculation, thereby causing a transition from a strong gel initiated by bridging flocculation to a weak gel due to steric stabilization overcoming the bridging flocculation.

Keywords: Silicon Carbide, Robocasting, Additive Manufacturing, Direct Ink Writing, Polyelectrolyte, Bridging Flocculation

Introduction

Direct ink writing is used for printing complex silicon carbide components for various applications. For direct ink writing, especially in robocasting printing technology, colloidal ink made of ceramic powder, polymer additives and water, is employed for fabrication of three-dimensional silicon carbide parts. The polymer additives are often polyelectrolytes. This process takes advantage of the steric hinderance due polymer interactions as well as the electrostatic forces exerted by the ions [1-2]. The process involves first forming a stable dispersion of aqueous colloidal suspension which is obtained by electrosteric stabilization process. Electrosteric stabilization is a combination of steric stabilization and electrostatic stabilization. Steric stabilization occurs as a result of steric hinderance when high-entropic polymer chains crowd a particle thereby preventing them from coming in close contact while electrostatic stabilization occurs due to electrical double layer of ions surrounding the particles, causing the particle to repel each other . The dispersion of colloidal suspension is followed by gelation or flocculation process [3]. This involves collapsing the electrical double layer responsible for repulsion between the particles as well as the steric hinderance that prevents the particles from sticking together. This is done in such a way that the particles are now weakly flocculated together. The idea behind gelation mechanism is to reduce the repulsive forces or steric hinderance between stabilized particles such that flocculation of the particles produces an interconnecting network of particles with high elastic modulus and sufficient yield stress needed to extrude ceramic paste successfully by robocasting.

The flocculation can be achieved by three different mechanisms: (i) a pH change, (iii) salt addition, and (iii) bridging flocculation [4]. In this present work, bridging flocculation is used for SiC colloidal ink design.

Bridging flocculation is the use of oppositely charged polyelectrolytes for colloidal ink formulation. Bridging flocculation occurs when polymer chain is absorbed onto the surface of more than one particle. The polymer chains then create a bridge or links between these particles, thereby turning the colloidal suspension into loose aggregates [5], or a weakly-flocculated gel. In the case of silicon carbide colloidal gel, previous research has shown that cationic polyelectrolyte is used as dispersant to obtain low-viscosity, well-dispersed silicon carbide colloidal suspension, and an anionic polyelectrolyte is used for flocculating the suspension into an elastic gel amenable to extrusion [6]. Cai *et al.* was the first to demonstrate the fabrication of complex 3D SiC structures using robocasting [6]. In their approach, an aqueous SiC was dispersed in a cationic polyelectrolyte, polyethylene Imine (PEI), viscosified by hydroxypropyl methyl cellulose (HMPC), and flocculated with an anionic polyelectrolyte, ammonium polyacrylate (APA). Subsequent works have either used similar approach or flocculate SiC suspension with pH [7]. Most of the works employed small SiC particle sizes, ranging from 40nm – 0.7μm, complimenting literature that finer powders are good for ink formulation because of better dispersion and sinterability, since larger particle size can easily agglomerate and be difficult to print [8]. Particle shape is also important. Spherical particles help facilitate ease of paste flowability due to the lower interparticle interaction and friction while platelet-like particles with irregular edges interact with each other, leading to agglomeration and thus nozzle clogging of ink even at low solid loading [8-10].

Milling process is usually done to obtain ceramic powders with better particle morphology and size for robocasting. The challenge still remains that most SiC colloidal ink is limited to low-moderate (30-44vol%) solid loading due to difficulty in printing with the nozzles. Even after milling the SiC using hardened steel, the ink was printed with 900μm nozzle [9]. Two challenges arise here: printing with low-to-moderate solid loading usually led to high shrinkage of sintered part. Secondly, printing with large nozzle sizes (600-1500μm) usually causes poor surface finish, warpage and distortion of the printed parts. Besides, smaller nozzle sizes in the range of 100-400μm are beneficial for intricate lattice structure, thin walls, fins and microchannels useful in heat-exchanger components, tiny porous scaffolds used in bone regeneration. To print highly concentrated SiC colloidal ink ~50vol% with smaller nozzle sizes requires optimizing the ink design. This work aims to develop a systematic approach for optimization of SiC colloidal ink by dual-polyelectrolyte ratio method, that is, the optimal ratio of the anionic to cationic polyelectrolyte. This optimal ratio can also ensure that this highly concentrated SiC colloidal ink is printed through small nozzle sizes to reduce surface roughness and also beneficial for intricate lattice structure, thin walls, fins and microchannels.

Materials and Methods

The primary constituent of the ceramic gel used in this study is silicon carbide powder with an average particle of 9.8 μm and theoretical density of 3.21 g/cm^3. An attrition milling process was carried out to reduce the particle size of the as-received powder. The powders were milled for 10 hours at 100 rev/s at a mass ratio of ~10:2:1 (ball to powder to water). A field emission scanning

electron microscope (SEM) was used to observe the particle morphology and shape of the as-received and milled SiC powder. The scanning was carried out with 10 KV for magnification 1000X, 2000X, and 10,000X.

SiC colloidal ink was initially formulated by adding the SiC powders to an aqueous polymer solution of 10 wt% high molecular weight polyethyleneimine (PEI) (0.0026 g/g SiC powders) in deionized water. PEI is a moderately charged cationic polyelectrolyte, which acts as a dispersant to create both an electrostatic repulsion and steric stabilization among the SiC particles. SiC powder was added in four steps with each step homogenized in a planetary centrifugal mixer for 1 min to obtain a stable dispersion of ceramic particles. A viscosifying agent, 5wt% hydroxypropyl methylcellulose (7 mg/mL liquid concentration, Methocel F4M, Mw= 3500 g/mol) is added to the suspension and mixed for 1 minute. The methylcellulose helps to increase the viscosity of the suspension and to prevent phase separation during ink extrusion. The final step in the colloidal gel preparation involves flocculation of the low-viscosity, well-dispersed PEI-coated SiC aqueous suspension with an opposing suitable polyelectrolyte, in this case, an anionic ammonium polyacrylate (APA) flocculant (0.008g/mL of liquid phase, Darvan-821), and then homogenized in a Thinky planetary mixer for 5 mins to ensure total homogeneity. The flocculant is added to make the gel strong by increasing its elasticity and viscosity. The final ink formulation containing a volume fraction of solids of 0.44 in proportion by weight percent is 71.61:21.99:3.97:1.86:0.57 for SiC powder, water, methylcellulose, PEI, and APA respectively. The initial, unoptimized dual-polyelectrolyte ratio (APA:PEI) is 1:3.27 for 44vol%. Table 1 shows the order in which the ink formulation was made, and weight proportion of SiC ink. The rheology of the ink depends on the concentration of each of the ink constituents. The resulting colloidal gel must flow through a small nozzle, and upon deposition the printed structure must retain the shape originally designed in the CAD model.

Table 1: Weight Proportion of SiC colloidal gel Constituents

S/N	Ink Constituents	Amount (g)	Weight proportion	Proportion by wt %
1	Mass of H2O	13.01	0.2199	21.99
2	Mass of PEI	1.102	0.0186	1.86
3	Mass of SiC	42.372	0.7161	71.61
4	Mass of HPMC	2.352	0.0397	3.97
	Mass of APA	0.336	0.0057	0.57

Optimization of SiC colloidal ink by dual-polyelectrolyte ratio approach

The objective here is to increase the solid fraction of SiC ceramic phase from 44vol% to 50vol%. This helps to improve the density and reduce the shrinkage of the final sintered part. It is also desired that this highly concentrated 50vol% SiC is printable with smaller nozzle diameter 250-410μm. The optimization process begins with a range of PEI dispersant concentrations. For the initial 44vol%, 8 different PEI concentrations were selected with an interval of about 0.1 to provide a good range of observations [see table 2]. The rheological test was carried out to determine the optimal PEI concentration for the dispersion stage. Having selected the optimal PEI concentration, the solid volume fraction was increased from 44vol% to 50vol%, and further

rheological tests were conducted to find out how increasing the solid fractions impact the viscosity of the suspension. Optimal dispersant for increased solid fractions was selected, and the final optimization step involved the selection of three different flocculant concentrations of anionic polyelectrolyte, APA. The optimal APA concentration is the one that gives the appropriate yield stress and elastic modulus suitable for printing with robocasting.

Rheological characterization of SiC colloidal ink

The rheological behavior of the inks was characterized using a controlled stress-strain rheometer (Model CVOR 200). A cup and bob geometry (cup I.D. =16 mm and bob O.D. = 14 mm) with serrated walls was used to prevent wall-slip. A custom-made solvent trap was also used to prevent evaporation of the sample during long periods required for rheological measurements. Two different types of measurements were carried out: (i) viscometry (ii) oscillatory stress sweep. Viscometry measures shear stress (τ) and apparent viscosity (η) of the inks as a function of shear rate (γ) using a shear rate range of $0.01 \leq \dot{\gamma} \leq 100s^{-1}$. Oscillatory stress sweep is used to measure the elastic (G') and the viscous (G'') shear modulus of the inks as a function of shear stress (τ). This helps to determine the yield and flow stress of the ink, and the linear viscoelastic region (LVR G'). The rheometer was operated in controlled stress mode with a shear stress range of $10 \leq \tau \leq$ 1000Pa. A non-linear least-squares regression fit of the viscometry data using Herschel-Buckley rheological model (1) done in MATLAB showed the values of yield stresses (τ_y), flow index (n), and consistency factor (K), where both the shear stresses (τ) and shear rates (γ) are known parameters given by the viscometry measurements.

$$\tau = \tau_y + K\dot{\gamma} \qquad (1)$$

For each measurement, the sample was loaded into the cup geometry using a syringe. The sample is allowed to rest or attain an equilibrium state for a period of 10-30 minutes before the first measurement was done and subsequently between each successive measurement. This is to eliminate the shear history undergone by the sample during the first initial pumping of the sample into the cup using a syringe and also to minimize the influence of the previous measurement on the next. For repeatability of the experiments, two batches of ink were made, and the measurements were replicated three times for each batch. The resulting data is a representation of the trends observed during the rheological measurements.

Results and Discussion

Effect of attrition milling on SiC particle morphology

Scanning Electron Microscope (SEM) showed that particle morphology of the as-received powders is characterized by irregular, flakey-like, sharp-edged structure, seen at different magnifications (1000, 2000 and 10000X) [Fig 1(a-c)]. This kind of particle morphology is not suitable for robocasting since the irregular shapes of the particles could cause interparticle interaction and friction to occur between the particles, thereby preventing easy and smooth extrusion through smaller nozzles. Secondly, the SEM [fig1(d-f)] revealed the particle morphology and shape of SiC powder after milling for 10 hours. Figure (1f) revealed a much smaller-sized, spongy-like particle. The particle morphology has significantly broken down from irregular flakes

into much smaller sizes below ~1μm average size, and that the edges of the particles are somewhat rounded off to facilitate the favorable particle interactions and ease of extrusion through smaller nozzles. Due to the smaller particle size, it is also expected this would facilitate improvement in density of the sintered 3D printed structure since smaller particles have better sinterability.

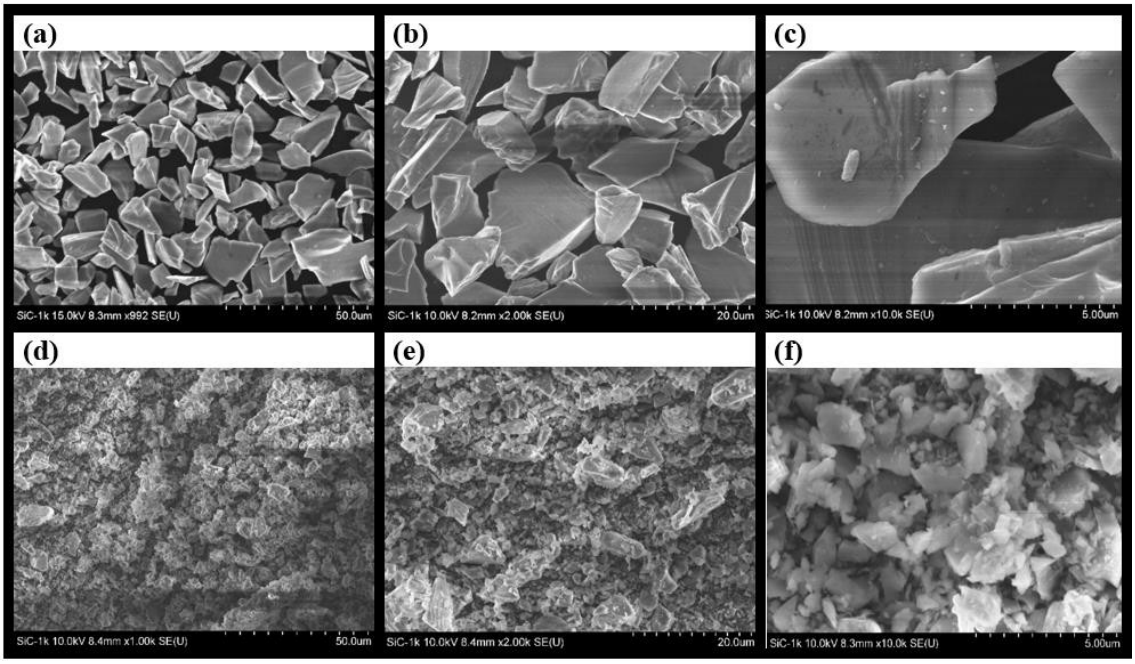

Figure 1: SEM images of as-received SiC powder in different magnifications: 1000X, 2000X and 10000X (a-c) and 10-hr milled powder at 1000X, 2000X and 10000X magnifications (d-f).

Determination of optimal dispersant concentration

Viscometry flow profiles showed that all of the PEI concentrations demonstrated shear-thinning behavior except for PEI-1 that deviated from shear-thinning to shear-thickening after a shear rate of $10s^{-1}$ [see fig.2]. While this shear-thinning behavior shows the viability of these inks for robocasting, only PEI-6, PEI-7, and PEI-8 demonstrated a much lower apparent viscosity suitable for robocasting. Therefore, these three PEI concentrations are examined for further optimization process.

The viscometry results were modeled in MATLAB using Herschel-Bulkley model, and the Herschel-Bulkley fit line showed that the lowest concentration of PEI (PEI-1) displayed a shear-thickening behavior [see fig. 3a], and that its flow index (n) is greater than 1, a characteristic of dilatant, shear-thickening fluid. PEI-2 shows a flow index (n) of ~1 which could either be a Newtonian fluid or a Bingham plastic [see table 2]. But since there was a yield stress, PEI-2 was said to exhibit Bigham plastic [see fig. 3a]. These deviations of PEI-1 and PEI-2 can be seen in fig. 3 where PEI-1 follows a characteristic dilatant curve and PEI-2 is a Newtonian fluid with a yield stress—a characteristic behavior of Bingham plastic fluid.

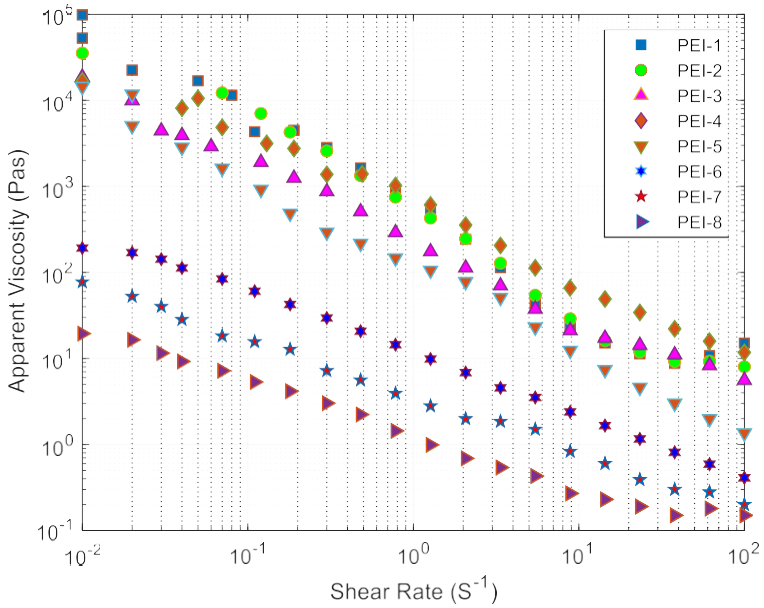

Figure 2: Apparent viscosity as a function of shear rate for 8 PEI concentrations [PEI-1-PEI-8]

Looking at the R^2 values, the Herschel-Bulkley could only model about 27% and about 1% of the data for PEI-1 and PEI-2, respectively, since they did not fit into the Herschel-Bulkley category of fluid. On the other hand, Herschel-Bulkley successfully modeled above 95% of the data for PEI-6, PEI-7, and PEI-8 with the model accounting for 99% variability of PEI-6. [see table 2]. Besides, PEI-6, PEI-7, and PEI-8 showed a pseudoplastic, shear-thinning behavior with little or not yield stress [see fig.3b]. The yield stress would be impacted by the flocculant during the gelation process.

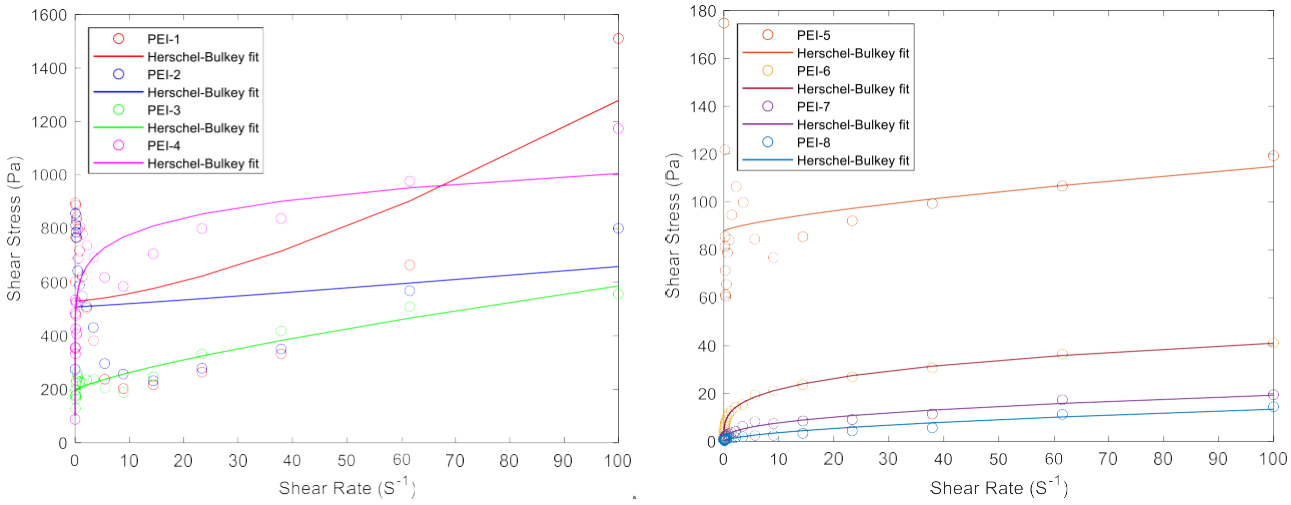

(a) (b)

Figure 3: Shear stress as a function of shear rate for 8 PEI concentrations (a) [PEI-1-PEI-4], (b) [PEI-5-PEI-8]

Table 2: Herschel-Bulkley Model Results for 8 PEI concentrations [PEI-1-PEI-8]

PEI	Concentration (g/gSiC)	PEI (g)	Flow Index (n)	R^2 Value	Yield stress (Pa)	Type of fluid
PEI-1	0.0062	0.263	1.44	0.276	530.01	Dilatant (shear-thickening)
PEI-2	0.0128	0.542	1.09	0.010	507.50	Bingham plastic (Non-shear-thinning)
PEI-3	0.0194	0.822	0.76	0.891	193.83	Nonlinear plastic (Shear-thinning)
PEI-4	0.0260	1.103	0.13	0.792	100.32	Nonlinear plastic (shear-thinning)
PEI-5	0.0326	1.381	0.72	0.066	87.82	Bingham plastic (shear-thinning)
PEI-6	0.0392	1.661	0.28	0.997	0	Pseudoplastic (shear-thinning)
PEI-7	0.0458	1.941	0.42	0.976	0.58	Pseudoplastic (shear-thinning)
PEI-8	0.052	2.220	0.57	0.956	0	Pseudoplastic (shear-thinning)

At a constant shear rate of $1s^{-1}$, the viscosity of each of the PEI dispersant concentrations was observed in a convergence curve. Figure 4 shows that the viscosity-PEI concentration curve converged at PEI-6, meaning that PEI-6 is the saturation point of the PEI in the suspension [see fig.4]. Beyond this, PEI-7 and PEI-8 are just excess polymer additives in the suspension which contributed nothing to further dispersion. Therefore, PEI-6 was selected as the optimal dispersant concentration for a low-viscosity, well-stable dispersion of SiC colloidal suspension.

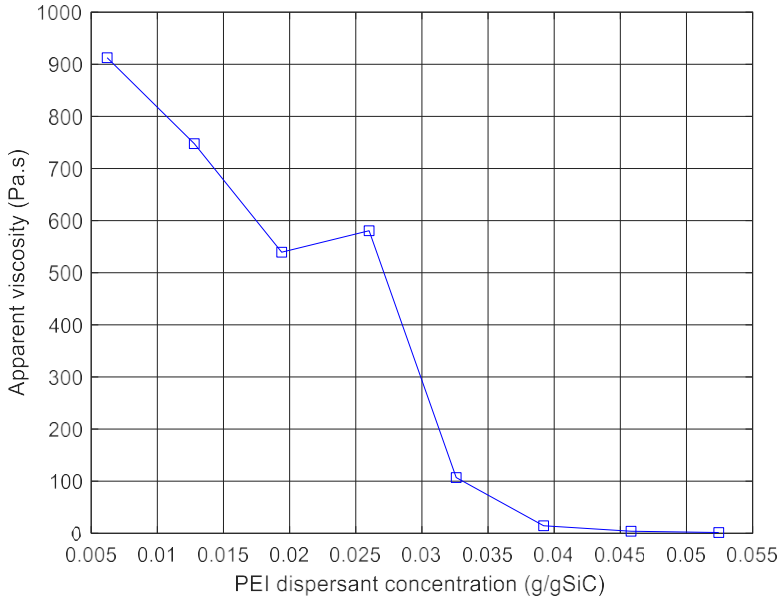

Figure 4: Apparent viscosity as a function of dispersant concentration [PEI-1-PEI-8]

Optimization of solids volume fraction of SiC

The solids volume fraction was gradually increased from 44vol% to 50vol%, and the effect of increasing solids volume fraction on the viscosity of SiC suspension is shown in figure 5. As expected, an increase in solids volume fraction increases the viscosity of the suspension. However, the variation in viscosity was not significant enough which means higher solids volume fraction did not cause significant increase in the viscosity. Therefore, it was determined that PEI-6 was still sufficient to disperse 50vol% fraction of silicon carbide, and thus was chosen was chosen as an optimal colloidal suspension ready for flocculation, and suitable for subsequent extrusion.

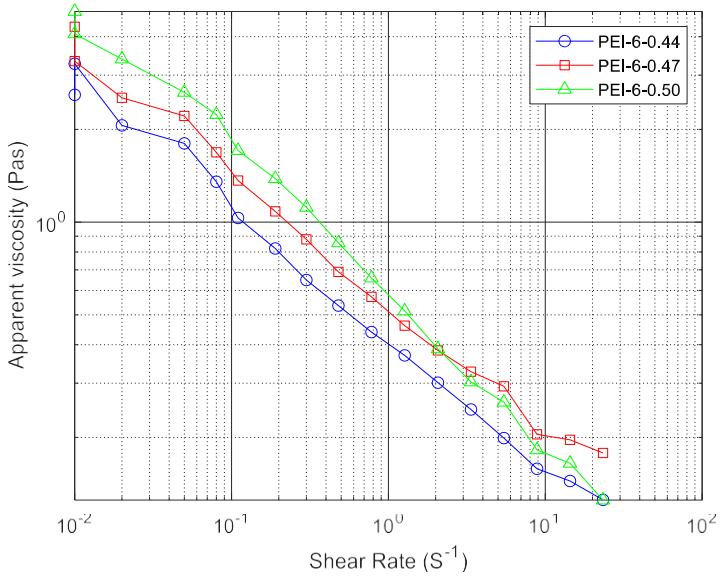

Figure 5: Apparent viscosity as a function of shear rate for three solid volume fractions [PEI-6-0.44, PEI-6-0.47, and PEI-6-0.50]

Optimization of flocculant for 50vol% solid fraction of SiC

Since the PEI-coated SiC suspension was too fluid to be extruded successfully by robocasting, it is important to flocculate or gel the suspension to be able to maintain the shape upon deposition. The amount of ammonium polyacrylate (APA), an anionic polyelectrolyte, which served as the flocculant were 0.143g, 0.216g, and 0.319g equivalent to concentrations of 0.0038, 0.0058, and 0.0085 (g/gSiC), and APA:PEI ratio of 1:11.6, 1:7.7, 1:5.2 designated with the terms APA-1, APA-2, and APA-3. The viscometry sweep test revealed that the three different concentrations exhibited a shear-thinning behavior, although APA-2 deviated from this shear-thinning behavior at shear rate above 10 s^{-1} [see fig. 7a]. The shear stress-shear rate curve in figure 8 revealed that both APA-1 and APA-3 demonstrated pseudoplastic, shear-thinning behavior with a flow index (n) of 0.16 and 0.37 [see table 3]. However, the highest amount of APA concentrations, APA-3, showed zero yield stress which is unsuitable for robocasting [see table 3]. Yield stress is necessary because it shows that upon deposition, the ink/paste would have enough resistance to deformation, and thus can retain its originally intended shape. Without yield stress, the paste might not be able to maintain a high number of layers before collapsing on the substrate. APA-1 showed

a significant amount of yield stress ~330Pa [see table 3]. This is a type of fluid described as yield-pseudoplastic fluid, also known as a nonlinear plastic fluid, which is the most suitable fluid for robocasting. While APA-2 also demonstrated a similar fluid behavior, there was a deviation from a shear-thinning behavior to shear-thickening behavior at about $10s^{-1}$ shear rate [see fig. 6b], making the Herschel-Bulkley model unable to explain the reason for the variability of about 99% of the data (R^2 value of ~0.2%) [see table 3], since this type of behavior cannot be modeled by Herschel-Bulkley fluid. Therefore, it can be concluded that APA-1 is the most suitable, and thus optimal APA concentration for SiC colloidal gel. Figure 6b supports this assertion by showing a good yield-pseudoplastic curve for APA-1, and that the R^2 value of 0.991 showed that the Herschel-Bulkley captures 99% of the data for APA-1, as opposed to 92% of APA-3.

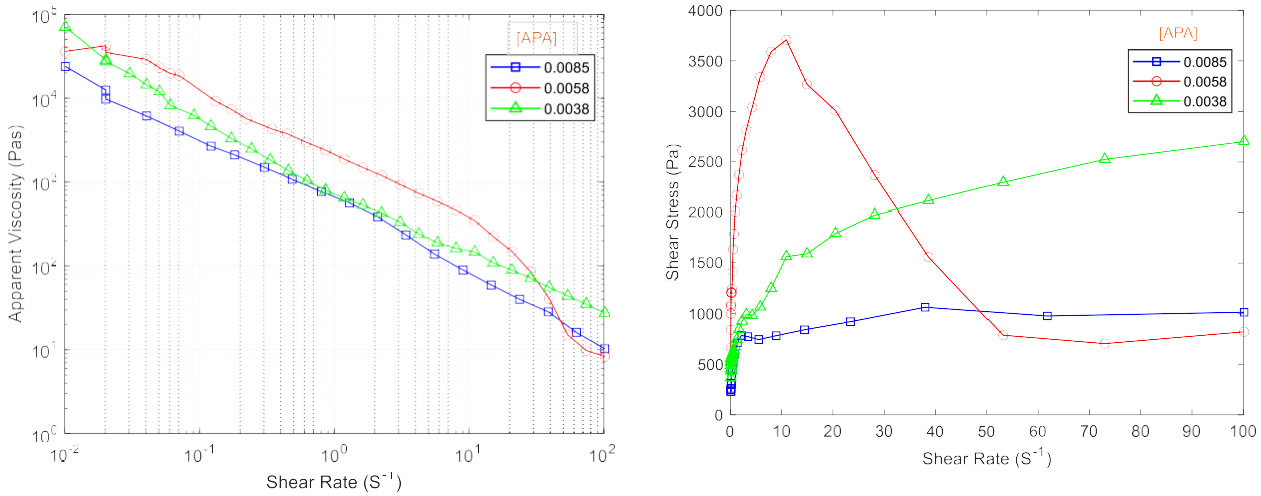

(a) (b)

Figure 6: (a) Apparent viscosity as a function of shear rate for APA flocculant concentrations [APA-1, APA-2, and APA-3],(b) Shear stress as a function of shear rate for APA flocculant concentrations [APA-1, APA-2, and APA-3].

Table 3: Herschel-Bulkley Model Results for 3 PEI concentrations [APA-1-APA-3]

APA	Concentration (g/gSiC)	APA(g)	Yield stress (Pa)	Flow index (n)	R^2
APA-1	0.0038	0.143	329.27	0.37	0.991
APA-2	0.0058	0.216	523.22	0.18	0.002
APA-3	0.0085	0.319	0	0.16	0.924

Viscoelastic Characterization of Silicon Carbide Colloidal Gel

APA-1 showed elastic modulus (G') of ~3 X 10^6 Pa in the linear viscoelastic region and a yield stress of ~183Pa. APA-2 showed an elastic modulus (G') of ~52 X 10^3 Pa in the linear viscoelastic region and a yield stress of ~42 Pa. APA-3 showed an elastic modulus (G') of ~35 X 10^3 Pa in the linear viscoelastic region and a yield stress of ~25 Pa [see table 4 & fig. 8]. APA-1 to APA-3 is an increasing order of APA concentrations, and it is expected that as the amount of

flocculant concentration increases, the elasticity (described by G') of the gel will increase. However, the opposite happened here, the elastic modulus and yield stress reduced as flocculant concentration increased. This is due to the fact that beyond 0.0038 (APA-1) concentration fraction, the amount of flocculant became too much that there was overcrowding of the polymer chains around the particle, leading to transition from bridging flocculation to steric stabilization which caused the depletion of the yield stress and elastic modulus. This explains the mechanisms by which polymers can act as a bridging flocculation agent at a low concentration and as a steric stabilizer at higher concentrations. This phenomenon has been described in other works [5]. For effective bridging flocculation, the polymer chains must not be attached to the entire surface of each particle because during Brownian collisions, further bridging flocculation occurs as the polymer chain segments attached to one particle can attach to the surface of another particle, thereby inducing continuous bridging flocculation. But if the polymer chain covers the entire surface of each colloidal particle, during Brownian collisions, instead of bridging flocculation only steric stabilization would take place since there is no room for polymer chain attached to one particle to attach to the surface of another particle [10]. In this case, polymer chains entropy reduces as the polymer chains segment hinders the movement of each other, and thus steric stabilization dominates. However, steric stabilization only provides little elasticity for colloidal gel insufficient for robocasting. Therefore, the flocculant concentration must be less than what is sufficient to cover the entire surface of a colloidal particle. That is why at a lower concentration of APA, there is a good network of particles which can store and release energy efficiently, attributed to its high yield strength and high elastic modulus (G'). This means that the ink can maintain its shape at a high number of layers without collapsing which is suitable for robocasting.

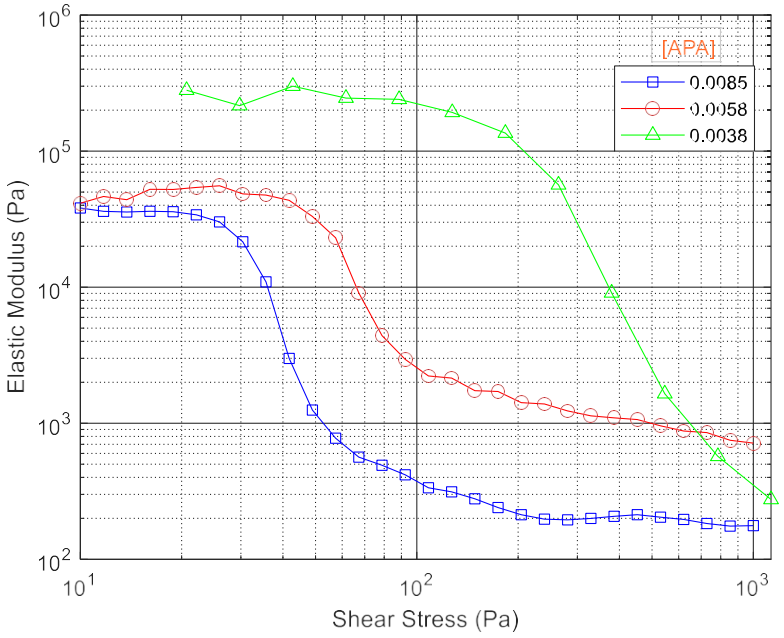

Figure 7: Elastic modulus as a function of shear stress for different APA concentrations [APA-1, APA-2, & APA-3]

The reduction in yield stress and elastic modulus at high concentration is due to the steric stabilization dominating over bridging flocculation which results in a less structured gel and thus required less stress to initiate flow; the system becomes more fluid-like than solid-like and less energy can be elastically stored, a typical behavior of APA-3. APA-2, on the other hand, is a complicated structure that probably has a combination of partial bridging flocculation and partial steric stabilization. At lower shear rate, the gel exhibited a shear-thinning behavior, as expected of the behavior of a typical yield-pseudoplastic fluid used in robocasting; however, beyond a shear rate of 10 s^{-1}, the behavior changed into a dilatant fluid. This is probably the point where steric stabilization began to dominate over bridging flocculation. Again, it can be concluded that APA-1 is the optimal flocculant concentration for SiC colloidal ink. Besides, in favor of APA-1, previous works have reported similar yield stress and elastic modulus for robocasting as the range of value for successful printing of colloidal gel by robocasting [6,9,11-12]. As a result, the optimal ratio of dual-polyelectrolyte [APA:PEI] for optimized 50vol% solid fraction of silicon carbide is 1:11.6.

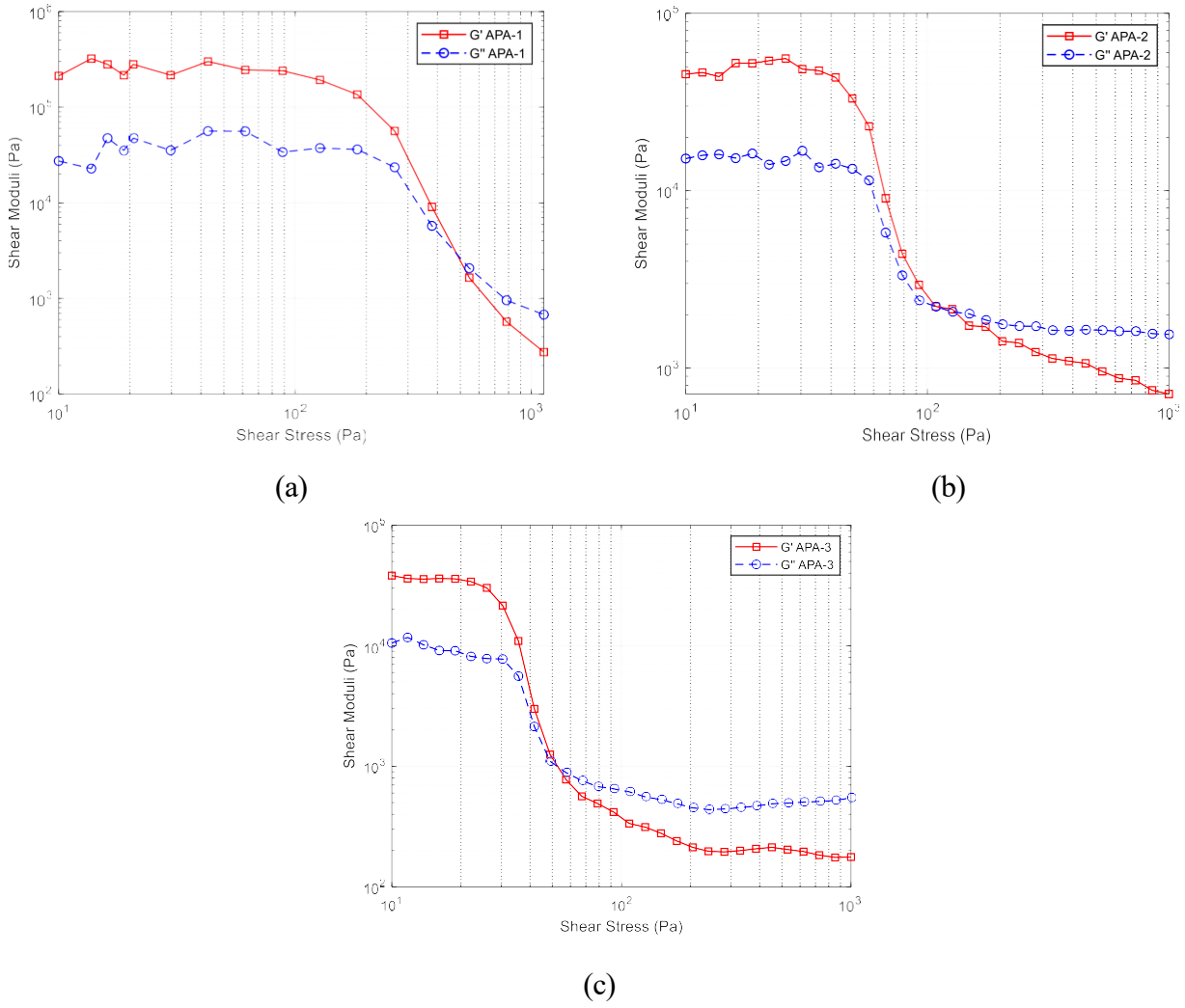

Figure 8: Elastic modulus (G') and viscous modulus (G'') as a function of shear stress for different APA concentrations (a) APA-1, (b) APA-2, and (c) APA-3

The viscoelastic behavior of SiC colloidal ink for three different APA concentrations are shown in figure 8, and it can be seen that all of the three exhibited viscoelastic behavior, that is, at some amount of stress known as flow stress, the ink transitioned from solid (elastic) behavior to liquid (viscous) behavior. Figure 8 shows that the viscous behavior became dominant after a flow stress of ~48Pa, ~126Pa, ~545Pa for APA-1, APA-2, and APA-3, respectively [see fig. 8 & table 4]. This kind of behavior is important in robocasting because it shows that during extrusion, once the shear stress is applied by the piston upon the paste in the syringe, the ink would transition to a liquid-like substance, aiding its flow through a very small nozzle by reducing its viscosity. However, it is expected that the ink should recover its elastic (solid) behavior immediately upon deposition.

Table 4: Viscoelastic Characterization of SiC ink for three different APA concentrations

APA	**Concentration (g/gSiC)**	**APA(g)**	**Mass ratio (APA:PEI)**	**LVR G'**	**Yield stress (Pa)**	**Flow stress (Pa)**
APA-1	0.0038	0.143	1:11.6	300,080	183.29	545.53
APA-2	0.0058	0.216	1:7.7	52,278	41.75	126.89
APA-3	0.0085	0.319	1:5.2	35688	25.93	48.94

Conclusion

The aim of this study is to develop a systematic approach toward optimization of SiC colloidal gel for direct ink writing process. For this purpose, the optimal ratio of flocculant to dispersant that enables the increase of solid volume fraction of SiC from 44vol% to 50vol% was investigated. The following conclusions are drawn from the study:

1. High concentration of dispersant is necessary for a low-viscosity, well-dispersed colloidal suspension. However, being too high may not necessarily contribute to dispersion and could just be excess dispersant.
2. For the initial, unoptimized ink formulation for 44vol% of SiC, the ratio of flocculant to dispersant was ~1:3 while the optimized ink formulation for 50vol% was ~1:11. This shows that in order to increase the SiC solid loadings by 6vol%, the amount of flocculant relative to dispersant must become significantly smaller, almost four times smaller.
3. Mass of high molecular weight PEI of 1.661g was determined as the optimal concentration of dispersant for silicon carbide, a significant increase from 1.102g used for the initial 44vol% formulation.
4. Increasing the amount of APA flocculant did not necessarily increase the yield strength and elastic modulus of the ink. In fact, increasing flocculant concentration had a reverse effect whereby the SiC ink transitioned from being gelled by bridging flocculation to steric stabilization, leading to reduced yield strength and elastic modulus. Therefore, the lowest APA concentration of 0.143g was determined as the optimal flocculant concentration for the gelation mechanism.

This presented approach demonstrates how volume of solid fractions can be increased by optimizing the ratio of flocculant to dispersant in the colloidal ink design. This approach will ensure that the final sintered part has lower shrinkage and higher density which is a subject of further investigation.

References

[1] J. E. Smay, G. M. Gratson, R. F. Shepherd, J. Cesarano, and J. A. Lewis, "Directed colloidal assembly of 3D periodic structures," *Advanced Materials*, vol. 14, no. 18, pp. 1279–1283, Sep. 2002, doi: 10.1002/1521-4095(20020916)14:18<1279::AID-ADMA1279>3.0.CO;2-A.

[2] J. CESARANO and I. A. AKSAY, "Processing of Highly Concentrated Aqueous α-Alumina Suspensions Stabilized with Polyelectrolytes," *Journal of the American Ceramic Society*, vol. 71, no. 12, pp. 1062–1067, 1988, doi: 10.1111/j.1151-2916.1988.tb05792.x.

[3] J. N. Stuecker, J. Cesarano, and D. A. Hirschfeld, "Control of the viscous behavior of highly concentrated mullite suspensions for robocasting," *J Mater Process Technol*, vol. 142, no. 2, pp. 318–325, Nov. 2003, doi: 10.1016/S0924-0136(03)00586-7.

[4] S. S. Nadkarni and J. E. Smay, "Concentrated barium titanate colloidal gels prepared by bridging flocculation for use in solid freeform fabrication," in *Journal of the American Ceramic Society*, Jan. 2006, pp. 96–103. doi: 10.1111/j.1551-2916.2005.00646.x.

[5] D. J. Growney *et al.*, "Star Diblock Copolymer Concentration Dictates the Degree of Dispersion of Carbon Black Particles in Nonpolar Media: Bridging Flocculation versus Steric Stabilization," *Macromolecules*, vol. 48, no. 11, pp. 3691–3704, Jun. 2015, doi: 10.1021/acs.macromol.5b00517.

[6] K. Cai *et al.*, "Geometrically complex silicon carbide structures fabricated by robocasting," in *Journal of the American Ceramic Society*, Aug. 2012, pp. 2660–2666. doi: 10.1111/j.1551-2916.2012.05276.x.

[7] S. Sun, Q. Xia, D. Feng, Z. Qin, and H. Ru, "Combining robocasting and alkali-induced starch gelatinization technique for fabricating hierarchical porous SiC structures," *Addit Manuf*, vol. 56, Aug. 2022, doi: 10.1016/j.addma.2022.102938.

[8] S. Lamnini, H. Elsayed, Y. Lakhdar, F. Baino, F. Smeacetto, and E. Bernardo, "Robocasting of advanced ceramics: ink optimization and protocol to predict the printing parameters - A review," *Heliyon*, vol. 8, no. 9. Elsevier Ltd, Sep. 01, 2022. doi: 10.1016/j.heliyon.2022.e10651.

[9] A. Jana *et al.*, "Effect of particle size on additive manufacturing of complex architecture of silicon carbide," *Ceram Int*, vol. 49, no. 11, pp. 17396–17404, Jun. 2023, doi: 10.1016/j.ceramint.2023.02.108.

[10] R. J. Hunter and L. R. White, *Foundations of Colloid Science*, no. v. 1. in Foundations of Colloid Science. Clarendon Press, 1987. [Online]. Available: https://books.google.com/books?id=GkJRAAAAMAAJ

[11] L. del-Mazo-Barbara and M. P. Ginebra, "Rheological characterisation of ceramic inks for 3D direct ink writing: A review," *Journal of the European Ceramic Society*, vol. 41, no. 16. 2021. doi: 10.1016/j.jeurceramsoc.2021.08.031.

[12] J. E. Smay, S. S. Nadkarni, and J. Xu, "Direct writing of dielectric ceramics and base metal electrodes," *Int J Appl Ceram Technol*, vol. 4, no. 1, pp. 47–52, Jan. 2007, doi: 10.1111/j.1744-7402.2007.02118.x.